

Silicate and labile DOC interfere in structuring the microbial food web via algal–bacterial competition for mineral nutrients: Results of a mesocosm experiment

*Harry Havskum*¹

Marine Biological Laboratory, University of Copenhagen, Strandpromenaden 5, DK-3000 Helsingør, Denmark

T. Frede Thingstad

Department of Microbiology, University of Bergen, Jahnebakken 5, N-5020 Bergen, Norway

Renate Scharek, Francesc Peters, Elisa Berdalet, M. Montserrat Sala, and Miquel Alcaraz

Institut de Ciències del Mar, CMIMA, Passeig Marítim de la Barceloneta 37–49, E-08003 Barcelona, Spain

Jan C. Bangsholt

The International Agency for ¹⁴C Determination, DHI, Agern Allé 11, DK-2970, Hørsholm, Denmark

Ulla Li Zweifel and Åke Hagström

Department of Biology and Environmental Science, Kalmar University, S-391 82 Kalmar, Sweden

Maite Perez and John R. Dolan

Marine Microbial Ecology Group, LOV UMR 7093 CNRS-UMPC, Station Zoologique, BP 28, F-06230 Villefranche-sur-Mer, France

Abstract

The effects of organic and inorganic nutrient enrichments on algal–bacterial competition were investigated using mesocosms. Interactions were followed over 10 d in 12, 3-m³ seawater mesocosms in the Isefjord, Denmark. Two sets of four mesocosms were given the same daily addition of “phytoplankton nutrients” (phosphate and nitrate) but received different amounts of glucose, and one set was kept in excess with respect to silicate. Four additional mesocosms served as controls and received either no additions, silicate alone, or glucose alone. In the mesocosm set where no silicate was added, enrichment with phytoplankton nutrients and glucose led to a replacement of diatoms, not by other algae, but by heterotrophic bacteria, mainly bacteria > 2 μm. In the mesocosm set where silicate was kept replete, diatoms competed successfully with bacteria for the uptake of mineral nutrients. Even in mesocosms enriched with high amounts of glucose, primary production increased throughout the experimental period, while bacterial production, after an initial increase, leveled off. In addition, turnover time of glucose increased in the silicate-replete mesocosm set, consistent with the idea that bacterial consumption was hampered by diatoms competing successfully for phosphate and nitrate. The size and shape of different algal and bacterial groups in relation to nutrient uptake and grazer avoidance are discussed. Both accumulation and consumption of dissolved organic carbon could depend on the structure of the microbial food web.

The common view of the role of heterotrophic bacteria is that of remineralizers, although it has long been recognized that bacteria utilize mineral nutrients (e.g., phosphate and ammonia). Furthermore, a large fraction of the uptake of

mineral nutrients can be in the bacterial size fraction (Harrison et al. 1977; Suttle et al. 1990). Thus, the idea that bacteria can compete with phytoplankton for mineral nutrients, rather than supply them as remineralizers, has been discussed for many years (Rhee 1972; Currie and Kalff 1984a,c; Bratbak and Thingstad 1985; Pengerud et al. 1987;

¹ Corresponding author (hhavskum@zi.ku.dk).

Acknowledgments

We thank Roskilde University Centre for equipping the laboratory at Sømminestationen in accordance with our needs. Special thanks to Hans Jørgen Olsen for his help with logistic problems at the station. For technical assistance, we thank Merete Allerup, Kristian Møller Christensen, Rita Muchitsch, and Alexandra Claudius Nielsen (The International Agency for ¹⁴C Determination), Evy Skjoldal (Department of Microbiology, University of Bergen), Berit L. Møller (National Environmental Research Institute of Denmark), and Mercedes Castaño (Institut de Ciències del Mar). Risø National

Laboratory, Denmark, is acknowledged for providing data on global radiation used for calculation of primary production. Two anonymous reviewers and the editor are acknowledged for their helpful suggestions.

This study was supported by MAST III (contracts MAS3-CT-0016-MEDEA and MAS3-CT-96-5034) and by the research project NTAP (contract EVK3-CT-2000-00022) of the EU RTD Programme “Environment and Sustainable Development” that forms part of the ELOISE projects cluster. It is ELOISE contribution 280/40.

Thingstad et al. 1993). Reports of mineral nutrient limitation of natural populations of heterotrophic bacteria (e.g., Elser et al. 1995) suggest that algal–bacterial competition could be an important element among mechanisms controlling the structure of the pelagic food web.

Comparing bacteria and algae, one would expect theoretically that bacteria, with their larger surface area to volume ratio and their higher growth potentials, could outcompete algae for dissolved inorganic nutrients such as N and P (Currie and Kalff 1984*a,b,c*). The trophodynamic situation is, however, complicated by the fact that the success of a population is the net result of both growth and loss processes.

A population with a low summed loss to predation, viral lysis, and sedimentation, can afford to grow slowly and still be the successful competitor in terms of biomass established. In this perspective, the role of large, grazer-avoiding, phytoplankton species such as chain-forming diatoms (e.g., *Skeletonema*), gelatinous colony-forming haptophytes (e.g., *Phaeocystis*), or filamentous cyanobacteria (e.g., *Nodularia*) becomes intriguing. Such phytoplankton, without necessarily being superior in their physiological abilities for nutrient uptake, but subject to relatively little grazing pressure from rapidly responding microzooplankton, could theoretically succeed in a nutrient-limited situation.

In an experimental context, diatoms are particularly interesting because their dependence on silicate permits experimental manipulation of their growth rates. Diatoms have considerably higher growth potentials than other algae when silicate is not limiting (Furnas 1990), and silicate addition is known often to stimulate diatom growth in natural communities (Egge and Aksnes 1992; Egge 1997).

Highly idealized representations of a food web consisting of heterotrophic bacteria, phytoplankton, and microzooplankton have proven successful in the analysis of nutrient-manipulated micro- and mesocosms (Thingstad et al. 1999*a,b*). The analyses suggest that the outcome of the competition between algae and heterotrophic bacteria (unlimited by either phosphorus or nitrogen) would be in favor of diatoms in the presence of excess silicate and in favor of bacteria given excess organic carbon and no silicate. Against this background, we present the results of a mesocosm experiment designed to examine the changes in the communities and activities of phytoplankton and bacterioplankton, subjected to different limitations.

Materials and methods

Study site, experimental setup, and sampling—The study was carried out from 15 to 27 June 1998 at a field station of Roskilde University Centre, Denmark, “Søminestationen,” at the Isefjord, 10 km east of Holbæk. Organic and inorganic nutrient enrichment experiments were performed in enclosures fixed to a pontoon bridge situated in the Isefjord (water depth 3 m; position, 55°42.78'N, 11°47.65'E). Each enclosure was filled with approximately 3 m³ of unfiltered surface water of the fjord during the evening of 15 June 1998.

The water column in these mesocosms was continuously circulated using an airlift that pumped the water from the bottom to the surface at a rate of 0.2 m³ h⁻¹. Nutrients were

Table 1. Summary of mesocosm treatment regimes. Numbers represent daily additions yielding final concentrations (mmol m⁻³). Silicate additions began on Day 3 when ambient silicate concentrations became undetectable in the mineral nutrient–enriched mesocosms.

Mesocosm	Phosphate	Nitrate	Glucose	Silicate
C ₀	0.1	1.6	0	0
C ₁	0.1	1.6	10.6	0
C ₃	0.1	1.6	31.8	0
C ₁₀	0.1	1.6	106	0
C ₀ Si	0.1	1.6	0	3.2–9.2
C ₁ Si	0.1	1.6	10.6	3.2–9.2
C ₃ Si	0.1	1.6	31.8	3.2–9.2
C ₁₀ Si	0.1	1.6	106	3.2–9.2
K _a	0	0	0	0
K _b	0	0	0	0
KC ₁₀	0	0	106	0
KSi	0	0	0	3.2/0

added between 2100 and 2200 h during the period 16–25 June 1998. The following nutrient manipulations, summarized in Table 1, were performed: eight mesocosms, all but four controls, the K set (i.e., K_a, K_b, KC₁₀, and KSi), received daily additions of nitrate as NaNO₃ and phosphate as KH₂PO₄ in Redfield ratio (1.6 mmol N m⁻³ and 0.1 mmol P m⁻³). These eight mesocosms represented two sets of increasing carbon addition (C₀, C₁, C₃, C₁₀) as glucose (0×, 1×, 3×, or 10× 10.6 mmol m⁻³). One set, the no-Si set (i.e., C₀, C₁, C₃, C₁₀), received no further additions, whereas silicate was added as Na₂SiO₃·9H₂O to the other set, the Si set (i.e., C₀Si, C₁Si, C₃Si, C₁₀Si) from Day 3, when the Si concentration in these enclosures fell below 3 mmol m⁻³. Si was subsequently kept in excess in the Si set (daily additions between 3.2 and 9.6 mmol m⁻³). Two controls (K_a and K_b) received no additions, and one control (KC₁₀) received daily additions of 106 mmol C m⁻³ and no other additions. In the fourth control (KSi), Si was kept in excess without any other additions. During the period 16–26 June 1998, water samples were collected daily from all 12 mesocosms between 0800 and 0900 h using transparent tubes (2 m long) to avoid zooplankton escape reactions. The salinity was 21.3 psu, and the water temperature varied between 15.3 and 17.9°C during the period.

To assure organic carbon in excess, some mesocosms received daily additions of 106 mmol glucose m⁻³ (i.e., C₁₀, and C₁₀Si), representing 10× the Redfield ratio compared to the added N and P. In natural environments, microbial populations might rarely encounter such high concentrations of a simple sugar. Rather than replicating a natural system, the high-glucose treatment was employed to help clarify the underlying mechanism of the competition between algae and bacteria when bacterial growth is not limited by organic carbon—for instance, after a sudden decay of a phytoplankton bloom releasing high amounts of dissolved organic carbon (DOC).

Nutrient analyses—Immediately after sampling, nutrient analyses were performed using an autoanalyzer. The analy-

ses for NO_2^- , NO_3^- (including NO_2^-), NH_4^+ , PO_4^{3-} , and SiO_4^- were performed according to Grasshoff et al. (1983).

Determination of bacterial production—Bacterial protein synthesis rates were measured using ^{14}C -leucine by applying the centrifugation method described by Smith and Azam (1992). For each determination, three replicates containing seawater only were incubated with ^{14}C -leucine ($100 \mu\text{mol m}^{-3}$) for 1 h in the dark at in situ temperature. Incubations were terminated by adding concentrated trichloroacetic acid (TCA) to a final concentration of 5%. In addition, two replicates that were treated with TCA (final concentration 5%) before addition of ^{14}C -leucine served as blanks. After incubation, all TCA-fixed samples were centrifuged, aspirated, and washed, and after addition of scintillation cocktail (OptiPhase "Highsafe 2," Wallac), the samples were counted in a scintillation counter (LKB Wallac 1214 Rackbeta). Incorporation rates of ^{14}C -leucine were converted to bacterial carbon production according to Simon and Azam (1989).

Determination of primary production—Maximum primary production was determined in situ by means of the acidification and bubbling procedure described by Riemann and Jensen (1991). Around noon, 4-h incubations were carried out using 20-ml glass vials, each containing 10-ml seawater samples with $2 \mu\text{Ci NaH}^{14}\text{CO}_3$ added (The International Agency for ^{14}C Determination, Denmark). The glass vials were incubated at light saturation depths ($300 \mu\text{mol photons m}^{-2} \text{ s}^{-1}$). The incubations were terminated by adding $500 \mu\text{l}$ formaldehyde (24.5%). After incubations, samples were treated with $100 \mu\text{l}$ 1 N HCl and bubbled for 24 h. Subsequently, 10 ml Instagel II Plus was added, and the samples were counted in a scintillation counter (LKB Wallac 1214 Rackbeta). Daily primary production was estimated from the light-saturated production (P_{max}); the photosynthetically available radiation at the surface, measured at hourly intervals; and the light extinction measured daily in the enclosures. Primary production was scaled to light intensity applying the equation $P(I) = P_{\text{max}} \tan h(I/I_s)$, where I is the depth-averaged light intensity in the depth intervals 0–1 and 1–2 m, respectively, and I_s is the light saturation constant (Jassby and Platt 1976). I_s was estimated in a separate experiment at $200 \mu\text{mol photons m}^{-2} \text{ s}^{-1}$ and used throughout the period.

Determination of mesozooplankton biomass—Water samples were filtered by gravity through $37\text{-}\mu\text{m}$ NITEX filters, and the filters plus the retained organisms were preserved in 4% formaldehyde buffered with hexamine. The volume filtered depended on the plankton concentration, which determined the clogging of the filter, and ranged between 3.25 and 13.5 liters. The filters with the retained organisms were gently washed and the organism suspension concentrated by settlement. Aliquots of the samples were studied under a stereomicroscope supplied with a CCTV camera connected to a computer. All mesozooplankton organisms present in the whole aliquot were included in images captured by means of a frame-grabber installed in a Macintosh. Organism volume was calculated by transferring the silhouettes of the organisms into surface-equivalent ellipses and calculat-

ing the volume of the resulting rotation ellipsoids. Carbon biomass was estimated from organism volume using conversion factors previously calculated from simultaneous measurements of volume (NIH-Image) and organic C (Carlo-Erba HNC analyzer) for coastal mesozooplankton (M. Alcaraz unpubl. data).

Determination of ciliate biomass—For ciliate enumeration, 50 ml of each water sample (preserved with acid Lugol's solution at 2% final concentration) were settled in standard settling chambers, and the entire bottom surface was scanned at $\times 200$ with an inverted microscope equipped with phase-contrast optics. Taxa were placed into two categories: (1) *Mesodinium rubrum* (Lohmann) Jankowski and (2) oligotrichs. Although *M. rubrum* has been reported to feed on cryptophytes (Gustafson et al. 2000), it is regarded as mainly phototrophic and was included in the phytoplankton compartment. The Lugol's fixative precluded identification of mixotrophic oligotrichs without distinctive gross morphologies (e.g., *Strombidium* spp.). Among oligotrichs, heterotrophic and mixotrophic oligotrichs were pooled and assigned to four subgroups according to their size and shape. For biovolume estimates, the average was calculated from the dimensions of at least 100 cells of each group or subgroup. Oligotrich biovolume estimates were converted to carbon using a factor of $0.2 \text{ pg C } \mu\text{m}^{-3}$ (Putt and Stoecker 1989).

Determination of colorless flagellate biomass—Samples were fixed with glutaraldehyde (2% final concentration), stained with 4'6-diamidino-2-phenylindole (DAPI), and filtered onto $0.8\text{-}\mu\text{m}$ black polycarbonate filters (Porter and Feig 1980). The filters were subsequently frozen and analyzed within 6 months. Flagellates $< 10 \mu\text{m}$ were enumerated in a Nikon Labophot-2 epifluorescence microscope at $\times 1,250$ magnification, whereas flagellates $> 10 \mu\text{m}$ were enumerated in a Leica DM RB epifluorescence microscope with $\times 600$ or $\times 1,000$ magnification. Between 200 and 400 cells were counted and sized per sample. Cells were assigned to one of four size classes based on cell diameter. To calculate cell volumes, dimensions of size classes dominated by naked flagellates were multiplied by a factor of 1.1 to compensate for shrinkage from fixation (Choi and Stoecker 1989). Cell volume (μm^3) was converted to cell carbon (pg) using a factor of $0.13 \text{ pg } \mu\text{m}^{-3}$, for classes that were dominated by thecate dinoflagellates, and $0.11 \text{ pg } \mu\text{m}^{-3}$ for all other flagellates (Mullin et al. 1966). Carbon biomass of the different groups was calculated from the cell density of each group and the carbon per cell content (Strathmann 1967).

Determination of diatom biomass—Samples were fixed with formaldehyde buffered with hexamine (0.6% final concentration) and enumerated using an inverted light microscope as described above for ciliates. For biomass estimations, diatoms were assigned either to one of three dominating species (*Skeletonema costatum* (Greville) Cleve, *Dactyliosolen fragilissimus* (Bergon) Hasle comb. nov., or *Chaetoceros curvisetus* Cleve) or to an "other diatoms" group. One of the dominant species, *S. costatum*, displayed varying cell dimensions, and individual cells were assigned to three subgroups according to their cell size (small, me-

dium, large). At least 100 cells of each group or subgroup were enumerated, and the dimensions of at least 20 cells were measured. The vacuole volume was subtracted from the cell volume (Hillebrand et al. 1999), assuming a plasma layer thickness of 1 μm (Strathmann 1967), and the remaining volume (μm^3) was converted to carbon content (pg) using a factor of 0.11 $\text{pg } \mu\text{m}^{-3}$ (Mullin et al. 1966). Carbon biomass was calculated as described above.

Determination of pigmented flagellate and picocyanobacteria biomass—Samples were fixed with glutaraldehyde (2% final concentration) and subsequently filtered onto black polycarbonate filters (pore size 0.2 μm for enumeration of picocyanobacteria and 0.8 μm for enumeration of pigmented flagellates, Porter and Feig 1980). The filters were frozen on the sampling day, stored at -30°C to preserve the chlorophyll autofluorescence (Porter and Feig 1980; Bloem et al. 1986; Sanders et al. 1989), and viewed within 6 months in a Leica DM RB epifluorescence microscope with $\times 600$ or $\times 1,000$ magnification. The organisms were assigned to 11 groups according to their size and taxonomic relationships (Havskum and Hansen 1997). At least 100 cells of each group in each sample were counted. Cell volume was calculated from the average cell dimensions of 100 cells in each group. The dimensions of naked flagellates were multiplied by a factor of 1.1 to compensate for shrinkage from fixation (Choi and Stoecker 1989). Cell volume (μm^3) was converted to cell carbon (pg) using the conversion factors of 0.22 $\text{pg C } \mu\text{m}^{-3}$ for picocyanobacteria (Søndergaard et al. 1991), 0.13 $\text{pg } \mu\text{m}^{-3}$ for thecate dinoflagellates, and 0.11 $\text{pg } \mu\text{m}^{-3}$ for all other flagellates (Mullin et al. 1966). Carbon biomass was calculated as described above.

Determination of bacterial biomass—Samples were treated like those described for colorless flagellates, except the filters used here had a pore size of 0.2 μm . Heterotrophic bacteria were differentiated into three groups: picobacteria ($< 2 \mu\text{m}$), colony-forming sausage-shaped bacteria (cell length 2–4 μm , colony diameter 20–60 μm), and filamentous bacteria (length up to 200 μm). At least 100 cells, colonies, or filaments of each group in each sample were counted. Cell volume was calculated from the average cell dimensions of 100 cells in each group. Cell volume was converted to cell carbon biomass by the factor 0.35 $\text{pg C } \mu\text{m}^{-3}$ (Bjørnsen 1986).

Turnover time for glucose (T_G)— T_G was measured in 20-ml samples incubated with ^{14}C -glucose. ^{14}C - CO_2 , and particulate ^{14}C $> 0.2 \mu\text{m}$ were collected according to a procedure modified after Hobbie and Crawford (1969). After incubation, the sample was split in two. Particulate uptake was measured on 10-ml samples filtered on 0.2- μm cellulose nitrate filters, and $^{14}\text{CO}_2$ was absorbed on 25-mm Whatman GF/F filters with 250 μl phenethylamine fixed inside the cap of 20-ml polyethylene scintillation vials containing the remaining 10 ml. T_G was calculated as the inverse of the fraction of added isotope consumed per hour.

DOC—DOC was measured using high-temperature catalytic oxidation (Sugimura and Suzuki 1988). DOC samples

were filtered through 0.2- μm filters (Gelman Supor) using disposable syringes (Terumo) connected to filter holders (Millipore) or by use of polycarbonate filtration units (Nalgene). Filtered water (7.5 ml) was transferred to polypropylene test tubes (Falcon, 15 ml) and immediately acidified with 100 μl of 1.2 $\mu\text{mol L}^{-1}$ HCl and kept at $+4^\circ\text{C}$ until analysis. All materials in contact with the samples, including the filters and filtration units, were carefully acid-rinsed with 1 $\mu\text{mol L}^{-1}$ HCl and washed with ultrapure water (Millipore Milli-Q) before use. DOC was measured with a high-temperature carbon analyzer (Shimadzu TOC 5000) using a four-point calibration curve with potassium biphtalate standard. Standard solutions were run at each analysis to check for instrumental shifts. Blanks were tested before each analysis by injection of ultrapure water. The total blank (Milli-Q water + system blank) was in all cases $< 10 \mu\text{mol C L}^{-1}$. Samples were not corrected for this blank. Triplicate injections showed standard deviations of 0–2%. At least two individually filtered samples were analyzed and showed standard deviations of 0–1% from the mean value of triplicate injections.

Statistical analyses—For bacterial and primary production, values were integrated over time for each mesocosm and then regression analyses were used to compare the no-Si set and the Si set. For the regression analyses, background levels of 8.5 $\text{mmol glucose m}^{-3}$ were assumed, according to reported average levels of glucose in surface seawater (Skoog et al. 1999).

We compared the biomass parameters within and between the no-Si set, the Si set, and the K set using analysis of covariance (ANCOVA) with sampling times as a covariate. Each treatment set was first tested for differences within. When no significant differences were recorded within a set, the mesocosms were used as replicates for the given biomass parameter, and the sets were compared using ANCOVA.

Among the various biomass parameters, there were differences within the sets for biomass of bacteria $> 2 \mu\text{m}$ and for biomass of the remaining algae (*see below*), thus preventing grouping into the major sets. For these parameters, as well as for the incomplete data set of ciliate biomass, groupings were made in the following way: (1) C_3 and C_{10} , (2) C_3Si and C_{10}Si , and (3) K_a and K_b . Although the controls were true replicates, C_3 and C_{10} , and C_3Si and C_{10}Si also were considered to be replicates, respectively, because the pairs were treated identically except for glucose addition and DOC accumulated in mesocosms with both $3\times$ and $10\times$ 10.6 mmol m^{-3} glucose addition (*see below*). In the case of turnover time of glucose, the time series were split into two halves (i.e., before and after Si depletion in the no-Si set), and mesocosm pairs C_0 and C_0Si , C_1 and C_1Si , C_3 and C_3Si , and C_{10} and C_{10}Si were analyzed separately. All statistical analyses were done with the software package Systat.

Results

Nutrient concentrations—Initial silicate concentrations were between 4 and 6 mmol m^{-3} in all mesocosms (Fig. 1). In the no-Si and the Si sets, silicate concentrations decreased, reaching between 1.7 and 3 mmol m^{-3} on Day 3.

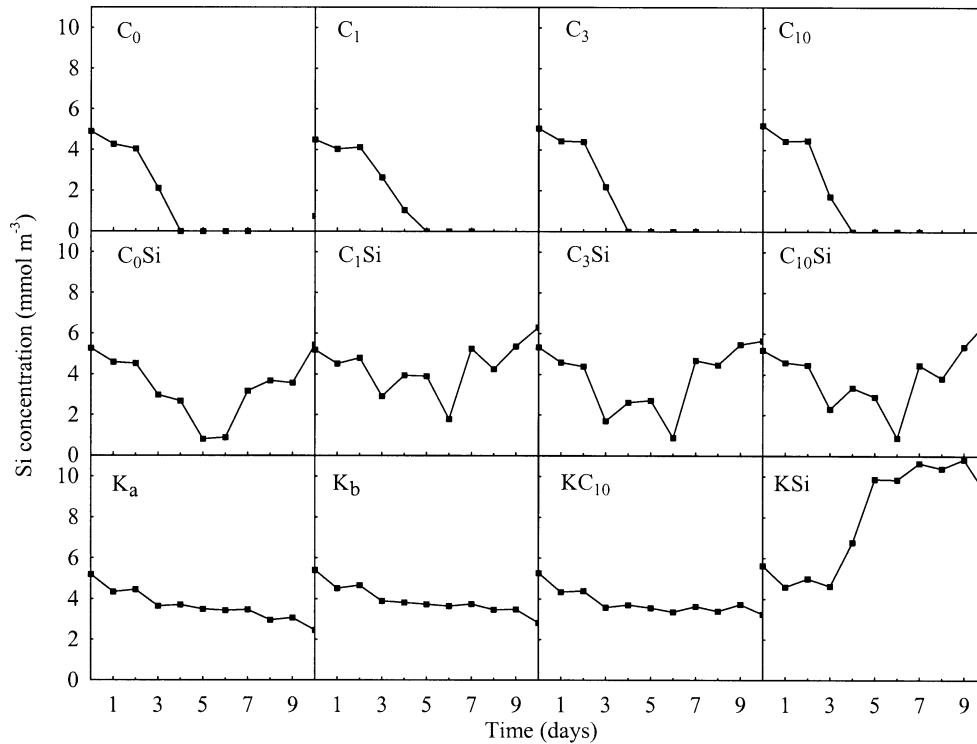


Fig. 1. Silicate concentration in the two nutrient-enriched mesocosm sets and in the controls. Upper panel, no-Si set without silicate enrichment and increasing carbon addition; middle panel, Si set with silicate enrichment and increasing carbon addition; lower panel, K set controls.

Thereafter, silicate concentrations fell below detection ($<0.71 \text{ mmol m}^{-3}$) in the no-Si set (Fig. 1). In the Si set, concentrations remained above detection, ranging between 0.8 and 6.6 mmol m^{-3} (Fig. 1). In the controls (K_a , K_b , and KC_{10}) silicate stayed between 2.8 and 4.7 mmol m^{-3} , whereas in the Si-amended control (KSi), silicate accumulated, reaching concentrations between 10 and 11 mmol m^{-3} (Fig. 1).

$\text{PO}_4\text{-P}$ and $\text{NO}_2\text{-N}$ were undetectable ($<0.16 \text{ mmol m}^{-3}$ and $<0.36 \text{ mmol m}^{-3}$ respectively) in all samples from all mesocosms (data not shown). $\text{NO}_3\text{-N}$ (including $\text{NO}_2\text{-N}$) was generally below detection ($<0.36 \text{ mmol m}^{-3}$), except in the no-Si and Si sets, which on Days 1 and 2 had concentrations ranging between 1.25 and 2.37 mmol m^{-3} (data not shown). $\text{NH}_4\text{-N}$ was below detection ($<0.36 \text{ mmol m}^{-3}$) or just above ($0.36\text{--}0.58 \text{ mmol m}^{-3}$) in all samples (data not shown).

Bacterial production—Addition of glucose alone (KC_{10}) increased bacterial production 3 d after the first addition from 22 to $44 \text{ mg C m}^{-3} \text{ d}^{-1}$, about two times the level of the controls without carbon addition (K_a , K_b , and KSi). The bacterial production in mesocosm KC_{10} then remained about two times as high as in the controls without carbon addition until the end of the study period, Day 10 (Fig. 2).

In mesocosms given mineral nutrients but no carbon (mesocosms C_0 and $C_0\text{Si}$), bacterial production increased 3 d after the first addition to about two times the level of the controls K_a and K_b . Subsequently, bacterial production continued to increase, reaching $150\text{--}250 \text{ mg C m}^{-3} \text{ d}^{-1}$ (about

eight times the level of the controls K_a and K_b) toward the end of the study period (Fig. 2).

Addition of both mineral nutrients and carbon (mesocosms C_1 , C_3 , C_{10} , and $C_1\text{Si}$, $C_3\text{Si}$, $C_{10}\text{Si}$) yielded increases in bacterial production after a lag phase of 1 d to between 140 and $390 \text{ mg C m}^{-3} \text{ d}^{-1}$ (about $8\text{--}23\times$ the level of the controls K_a and K_b) on Day 2. On Day 3, bacterial production continued to increase in all mesocosms enriched with both mineral nutrients and carbon. Subsequently, bacterial production decreased to the level of Day 2 and remained at that level in these mesocosms until the end of the study period, except for mesocosms C_3 and C_{10} , where a second and even higher peak was observed toward the end of the study period reaching between 740 and $840 \text{ mg C m}^{-3} \text{ d}^{-1}$ (Fig. 2). Standard deviation between internal replicates never exceeded 5% (data not shown).

Integrated bacterial production increased significantly with increasing glucose enrichment both with and without Si enrichment ($p < 0.01$ in both cases). The increase was, however, significantly lower in the Si set than in the no-Si set ($p < 0.05$) (Fig. 3).

Primary production—Initially $70\text{--}120 \text{ mg C m}^{-3} \text{ d}^{-1}$, primary production increased in all mesocosms during the first day between 20 and 80% (Fig. 2). Although it subsequently decreased or leveled off in the K set, it continued to increase in the no-Si set and the Si set until Day 5, reaching values between 590 and $1,200 \text{ mg C m}^{-3} \text{ d}^{-1}$ (Fig. 2). Thereafter, primary production leveled off in mesocosm C_0 (Fig. 2). It

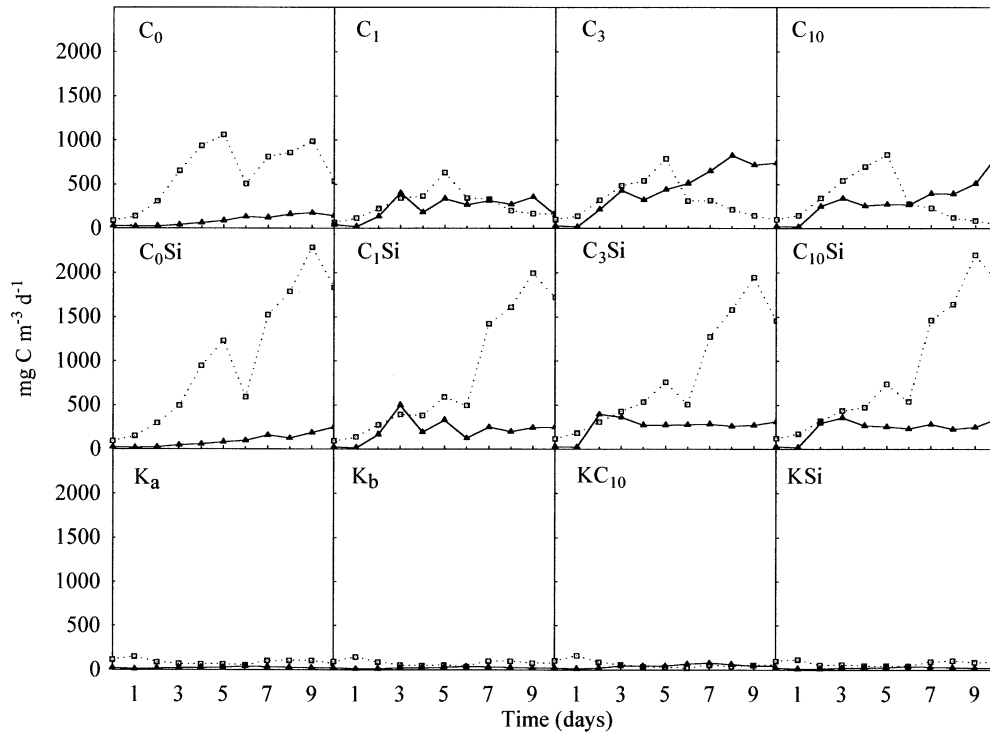


Fig. 2. Primary production (dotted line with open squares) and bacterial production (solid line with filled triangles) in the two nutrient-enriched mesocosm sets and in the controls. Upper panel, no-Si set without silicate enrichment and increasing carbon addition; middle panel, Si set with silicate enrichment and increasing carbon addition; lower panel, K set controls.

declined to $170 \text{ mg C m}^{-3} \text{ d}^{-1}$ in mesocosm C_1 , to $100 \text{ mg C m}^{-3} \text{ d}^{-1}$ in mesocosm C_3 , and to $54 \text{ mg C m}^{-3} \text{ d}^{-1}$ in mesocosm C_{10} (Fig. 2). In contrast, in the Si set, primary production continued to increase after Day 5, reaching values between $1,900$ and $2,300 \text{ mg C m}^{-3} \text{ d}^{-1}$ (Fig. 2). Standard deviation between internal replicates never exceeded 5% (data not shown).

In the Si set, the integrated primary production was significantly higher than in the no-Si set ($p < 0.01$) (Fig. 4). Although there was a trend for decreasing integrated primary

production with increasing carbon addition (Fig. 4), it was not statistically different for either the Si set ($p = 0.169$) or the no-Si set ($p = 0.061$).

Biomass of mesozooplankton, ciliates, and colorless flagellates—Mesozooplankton biomass increased significantly over time in all mesocosms ($p < 0.01$), including the controls, from an initial average of 78 mg C m^{-3} to, on average, 230 mg C m^{-3} at the end of the period. No significant difference within ($p = 0.359$) and between ($p = 0.370$) the

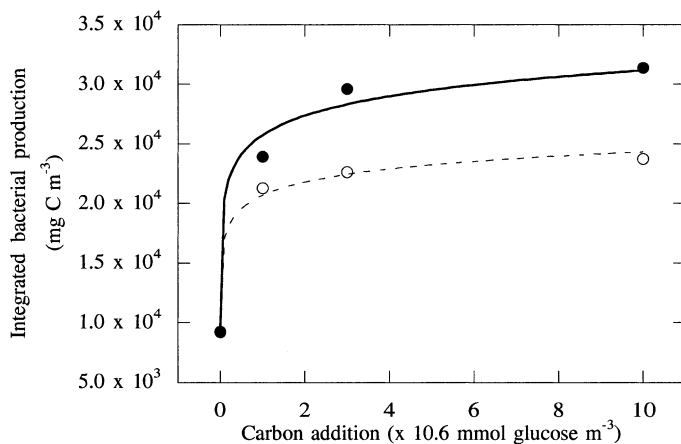


Fig. 3. Logarithmic regression of bacterial production integrated over time. No-Si set, solid line; Si set, broken line.

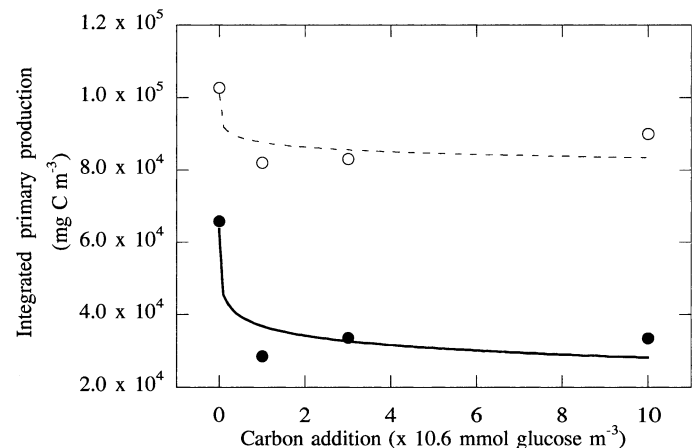


Fig. 4. Logarithmic regression of primary production integrated over time. No-Si set, solid line; Si set, broken line.

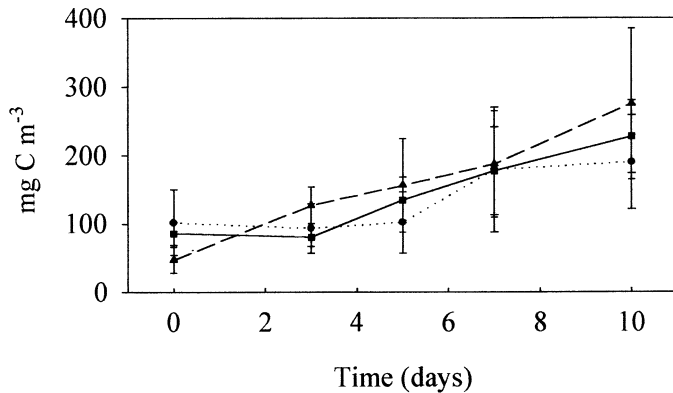


Fig. 5. Mesozooplankton biomass. Average from different treatments with standard deviation. Broken line with triangles, no-Si set (C_0 , C_1 , C_3 , C_{10}); dotted line with circles, Si set (C_0 Si, C_1 Si, C_3 Si, C_{10} Si); solid line with squares, K set (K_a , K_b , KC_{10} , KSi).

three sets (i.e., the no-Si set, the Si set, and the K set) were observed (Fig. 5). The largest size classes were composed of neritic copepods that were considerably smaller than oceanic copepods (data not shown).

Ciliate biomass peaked in the middle of the study period in all mesocosms. Maximum values were between 27 and 76 mg C m⁻³ in the mineral nutrient-enriched mesocosms and between 15 and 21 mg C m⁻³ in the controls (K_a , K_b ,

KC_{10} , Fig. 6). Initial and final biomasses were similar, between 0.4 and 13 mg C m⁻³ in all mesocosms (Fig. 6). Because the ciliate data set was incomplete, the controls K_a and K_b were compared with C_3 and C_{10} , and C_3 Si and C_{10} Si. No significant difference in ciliate biomass between the controls and the nutrient-enriched mesocosms with and without silicate addition was found ($p = 0.243$).

The initial biomass of the <10- μ m colorless flagellates decreased in all mesocosms during the first days from above to below 50 mg C m⁻³ (Fig. 6). Subsequently, their biomass tended to increase again at the end of the study period in the no-Si set and the Si set, but not in the K set (Fig. 6). Although the biomass of colorless flagellates <10 μ m was similar in the no-Si and Si sets (average 53.4 and 55.9 mg C m⁻³, respectively), it was significantly lower ($p < 0.01$) in the K set (average 34.8 mg C m⁻³).

The biomass of colorless dinoflagellates and other colorless flagellates >10 μ m increased in all mesocosms (Fig. 6). In the no-Si and Si sets, the biomass increased from <20 mg C m⁻³ to between 80 and 130 mg C m⁻³ without a significant difference between them (average 58.8 and 51.2 mg C m⁻³, respectively). In contrast, in the K set, the biomass of colorless flagellates >10 μ m remained significantly lower (average 18.9 mg C m⁻³, $p < 0.01$) and never exceeded 50 mg C m⁻³ (Fig. 6).

The colorless flagellates <10 μ m (*Telonema*, *Leucocryp-*

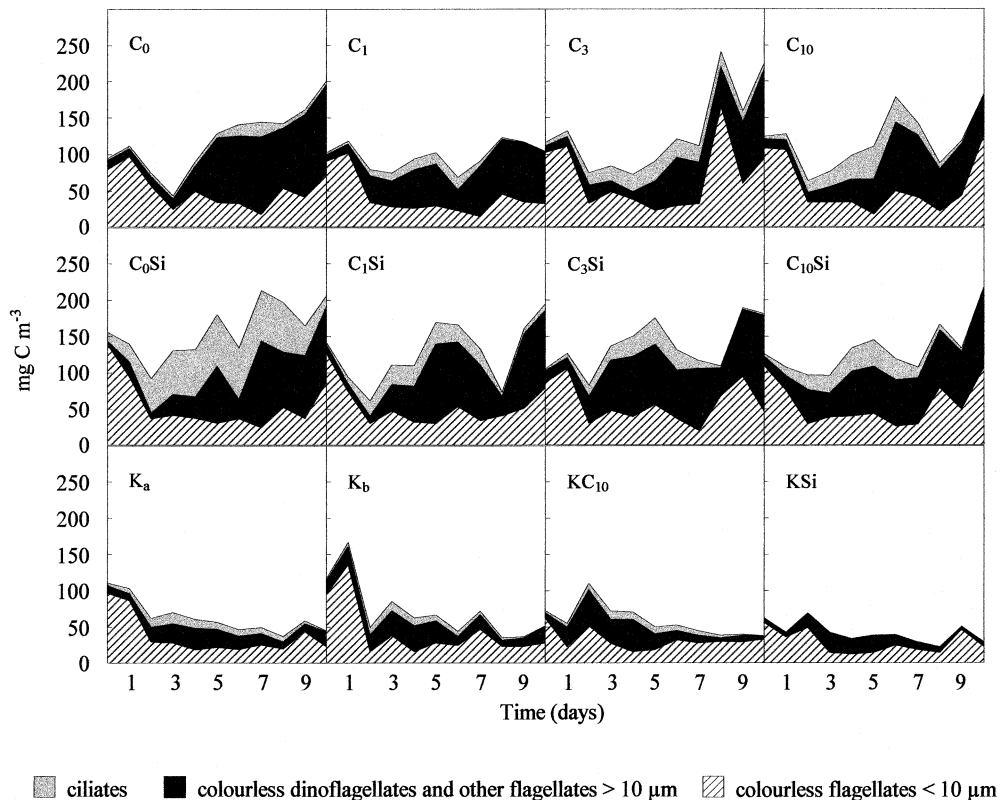


Fig. 6. Biomass of phagotrophic protists in the two nutrient-enriched mesocosm sets and in the controls. Upper panel, no-Si set without silicate enrichment and increasing carbon addition; middle panel, Si set with silicate enrichment and increasing carbon addition; lower panel, K set controls. Ciliate biomass not determined in KSi.

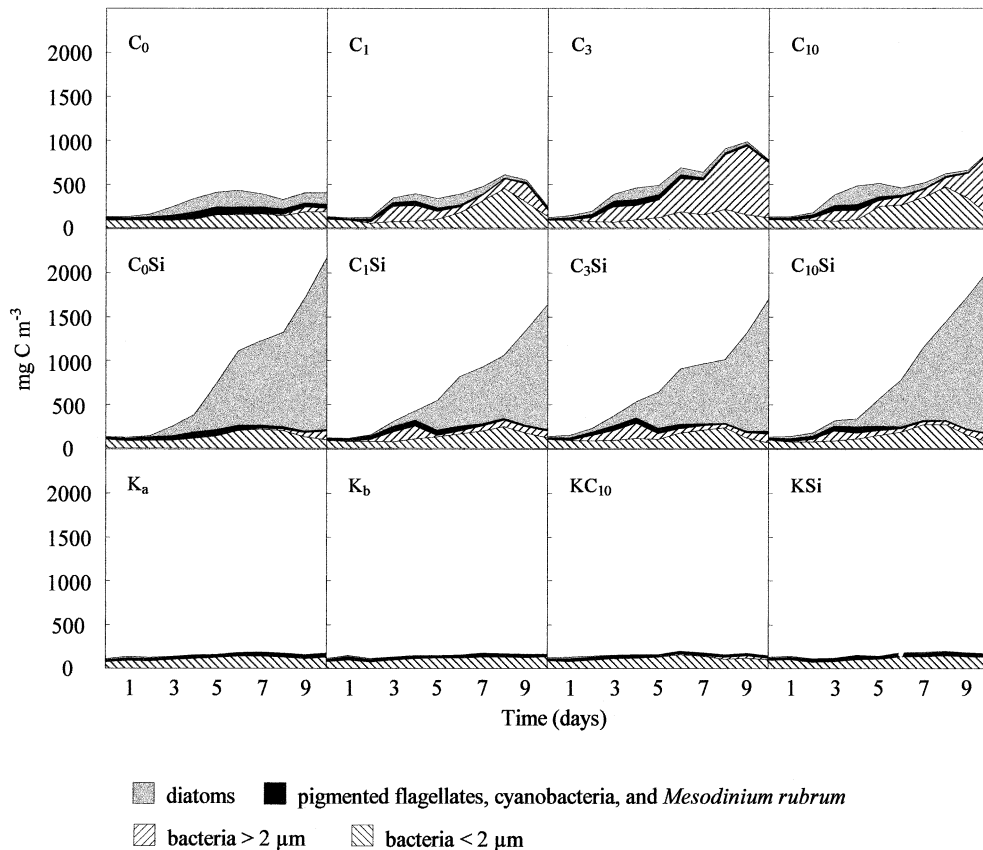


Fig. 7. Algal and bacterial biomass in the two nutrient-enriched mesocosm sets and in the controls. Upper panel, no-Si set without silicate enrichment and increasing carbon addition; middle panel, Si set with silicate enrichment and increasing carbon addition; lower panel, K set controls.

tos, choanoflagellates, and others) were feeding mainly on picoplankton, whereas the colorless flagellates $>10 \mu\text{m}$ (dinoflagellates and *Ebria* sp.) were feeding on larger organisms (H. Havskum unpubl. data from uptake experiments using fluorescently labeled prey).

Algal and bacterial biomass—Initially, the bacterial biomass (between 78 and 110 mg C m^{-3}) was approximately three times higher than the algal biomass (between 24 and 40 mg C m^{-3}) in all mesocosms (Fig. 7). Bacteria $>2 \mu\text{m}$ (filamentous and colony-forming bacteria) accounted for $<2.3\%$ of the bacterial biomass (Fig. 7). Diatoms accounted for between 14 and 40% of the algal biomass (Fig. 7). In the K set, the bacterial biomass stayed between 76 and 150 mg C m^{-3} and the algal biomass between 24 and 46 mg C m^{-3} throughout the study period (Fig. 7). In contrast, profound changes occurred in the no-Si and Si sets.

Until Day 4, algal biomass increased in the two sets to between 130 and 280 mg C m^{-3} (Fig. 7). Diatoms increased to between 57 and 77% of the algal biomass. From Day 4 on, silicate became depleted in the no-Si set (Fig. 1). Algal biomass leveled off in C_0 and decreased to $<40 \text{ mg C m}^{-3}$ in the mesocosms C_1 , C_3 , and C_{10} (Fig. 7). Very different trends were evident in the Si set. Algal biomass continued to increase, reaching between 1,500 and $2,000 \text{ mg C m}^{-3}$

with diatoms accounting for between 98 and 99% of algal biomass (Fig. 7).

Diatom biomass was dominated by *S. costatum*, *D. fragilissimus*, and *C. curvisetus*, forming chains up to 1 mm in length (data not shown). Diatom biomass was significantly higher ($p < 0.01$) in the Si set (548 mg C m^{-3}) compared to the no-Si set (68.9 mg C m^{-3}) and the K set (5.4 mg C m^{-3}).

The remaining algae were picocyanobacteria, pigmented flagellates $<10 \mu\text{m}$, and the mainly photoautotrophic ciliate *M. rubrum* (Fig. 7). The biomass of the remaining algae was not significantly different within the Si set, but within the no-Si set, the biomass in C_0 (57.7 mg C m^{-3}) was significantly higher ($p < 0.01$) than in C_1 , C_3 , and C_{10} (average 32.3 mg C m^{-3}). When the biomass of the remaining algae of the controls (K_a and K_b) was compared with that of the nutrient-enriched mesocosms with and without silicate addition (C_3 and C_{10} , and $C_3\text{Si}$ and $C_{10}\text{Si}$), no significant difference was found ($p = 0.763$).

Bacterial biomass increased dramatically in mesocosms with carbon but no silicate additions (C_1 , C_3 , and C_{10}), reaching maximum values between 560 and 940 mg C m^{-3} (Fig. 7). In mesocosm C_0 and in the Si set, bacterial biomass increased much less, reaching maximum values between 230 and 320 mg C m^{-3} (Fig. 7). Bacteria $>2 \mu\text{m}$ accounted for

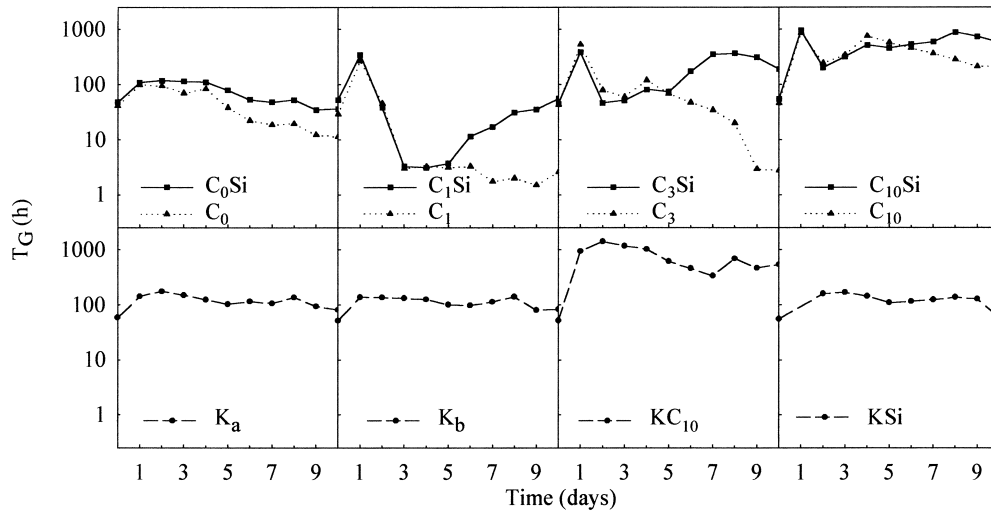


Fig. 8. Turnover time of glucose (T_G) for the no-Si and Si sets (upper panel) and for the K set (lower panel).

a large share of the bacterial biomass in the carbon- and mineral nutrient-enriched mesocosms without silicate enrichment (i.e., 20% in mesocosm C_1 , 34% in mesocosm C_3 , and 84% in mesocosm C_{10} at the end of the study period, Fig. 7). Colony-forming bacteria (cell length = 3 μm , cell width = 1 μm , and colony diameter = 20–60 μm) accounted for the major part of the $>2\text{-}\mu\text{m}$ bacteria; filamentous bacteria (length up to 200 μm) never exceeded 10% of the biomass of $>2\text{-}\mu\text{m}$ bacteria (data not shown).

Because the biomass of bacteria $>2\text{ }\mu\text{m}$ showed internal differences within the no-Si, the Si, and the K sets, these mesocosms could not be grouped for statistical analyses of this biomass parameter. In the mesocosms C_3 and C_{10} , the biomass of bacteria $>2\text{ }\mu\text{m}$ (average 230 mg C m^{-3}) was significantly higher ($p < 0.001$) than in mesocosms $C_3\text{Si}$ and $C_{10}\text{Si}$ (average 56.0 mg C m^{-3}), where the biomass in turn was significantly higher ($p < 0.001$) than in mesocosms K_a and K_b (average 1.67 mg C m^{-3}) (Fig. 7).

The biomass of bacteria $<2\text{ }\mu\text{m}$ was not significantly different in the no-Si set (average 156 mg C m^{-3}) and the Si set (average 134 mg C m^{-3}), but in the K set (average 114 mg C m^{-3}), the biomass was significantly lower ($p < 0.01$) (Fig. 7).

At the end of the experiment, the ratio of algal to bacterial biomass differed considerably in the no-Si and Si sets. In the absence of silicate additions, bacterial biomass compared to algal biomass was $\sim 1.3\times$ larger in mesocosm C_0 , $5\times$ larger in mesocosm C_1 , $24\times$ larger in mesocosm C_3 , and $35\times$ larger in mesocosm C_{10} . In the Si set, algal biomass dominated, representing between $7.5\times$ and $12\times$ the biomass of bacteria (Fig. 7).

Turnover time for glucose—Low values of T_G , indicating rapid turnover rates for glucose, would be expected in situations where the bacterial growth rate is carbon-limited and glucose is therefore depleted, whereas long turnover times would occur when bacterial growth rate is mineral nutrient (e.g., N or P)-limited and the added glucose accumulates. Results in mesocosm pairs that received identical treatment

until Si addition started (i.e., C_0 and $C_0\text{Si}$, C_1 and $C_1\text{Si}$, C_3 and $C_3\text{Si}$, and C_{10} and $C_{10}\text{Si}$, respectively), paralleled each other closely up to Day 5 (Fig. 8, upper panel) without significant differences. Thereafter, a consistent effect of Si was observed with a split in each pair. In all pairs, glucose turnover times in the Si-replete mesocosms increased significantly relative to their corresponding Si-depleted mesocosms C_0 and $C_0\text{Si}$ ($p < 0.0001$), C_1 and $C_1\text{Si}$ ($p < 0.01$), C_3 and $C_3\text{Si}$ ($p < 0.01$), and C_{10} and $C_{10}\text{Si}$ ($p < 0.05$). The observed split was consistent with the hypothesized effect of silicate availability on glucose utilization. The particular difference observed from Day 2 with higher T_G in mesocosms without added glucose (C_0 and $C_0\text{Si}$) than in those receiving $1\times$ Redfield ratio in glucose-C (C_1 and $C_1\text{Si}$) is interpreted by us as indicating a C-limited bacterial growth rate in the initial water and throughout the experiment in C_0 and $C_0\text{Si}$. Addition of glucose thus presumably increased uptake rate while concentration remained low, resulting in a reduced T_G (Fig. 8, upper left). In the controls (K_a , K_b , and $K\text{Si}$), T_G remained constant, whereas it increased in KC_{10} after glucose addition (Fig. 8, lower panel).

DOC—DOC accumulated only in the enclosures with $3\times$ and $10\times$ glucose enrichment (C_3 , C_{10} , $C_3\text{Si}$, $C_{10}\text{Si}$, and KC_{10} , Fig. 9). At the end of the study period, DOC concentration decreased to the initial level in C_3 , but not in $C_3\text{Si}$ (Fig. 9). In C_{10} , the DOC concentration leveled off toward the end, whereas it continued to increase in $C_{10}\text{Si}$ (Fig. 9).

Discussion

We found that the phytoplankton did not bloom in all mesocosms that were nutrient (N and P)-enriched (Fig. 7). If Si became depleted and C was added, the large diatoms became Si-limited, and the smaller phytoplankton groups could not compete with mineral nutrient-limited bacteria. In these mesocosms, bacterial biomass was dominated by cells 3 μm in length that formed colonies 20–60 μm in diameter. Because of their size, these bacteria were not suitable as prey

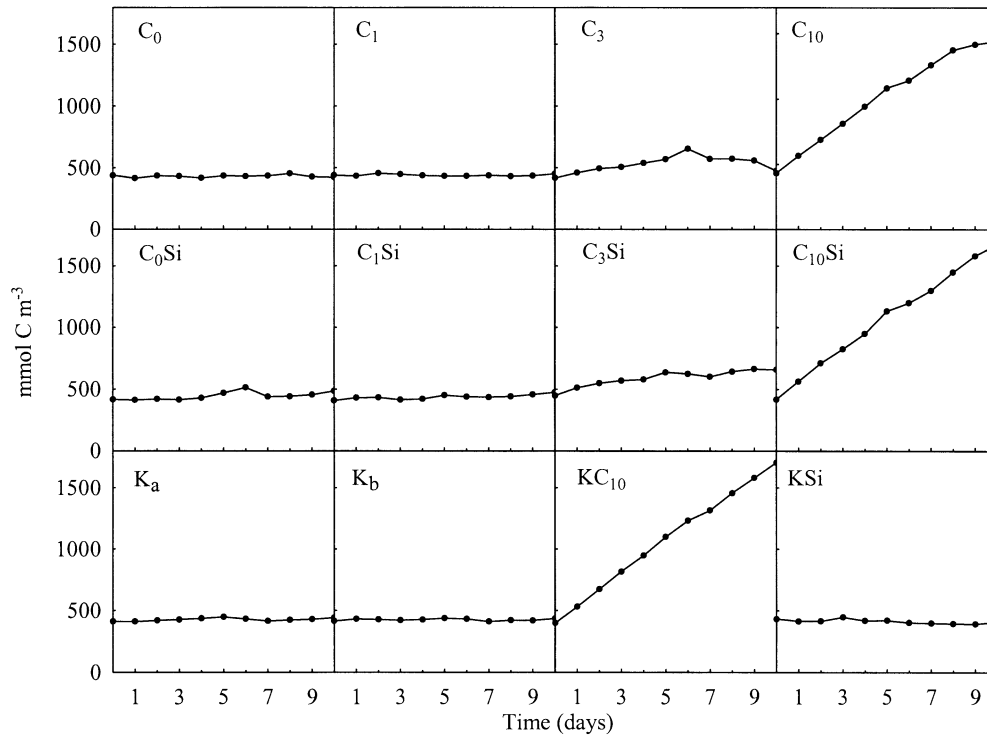


Fig. 9. DOC concentration in the two nutrient-enriched mesocosm sets and in the controls. Upper panel, no-Si set without silicate enrichment and increasing carbon addition; middle panel, Si set with silicate enrichment and increasing carbon addition; lower panel, K set controls.

for fast-growing bacterivorous nanoflagellates. Bacterial production exceeded primary production considerably, and algae were replaced by bacteria (Figs. 2, 7).

Similarly, integrated values of bacterial and primary production showed opposite patterns in the two mesocosm sets with increasing glucose addition: Integrated bacterial production increased with increasing glucose addition but was significantly higher in the no-Si set than in the Si set (Fig. 3). In contrast, integrated primary production was significantly lower in the no-Si set than in the Si set (Fig. 4).

Considering the two sets of Si and no-Si mesocosms, it is striking that the biomass of bacteria $< 2 \mu\text{m}$, colorless flagellates $< 10 \mu\text{m}$, colorless dinoflagellates and other colorless flagellates $> 10 \mu\text{m}$, and mesozooplankton showed no significant differences (Figs. 5–7). In addition, the biomass of algae other than diatoms and the biomass of ciliates were not significantly different between mesocosms with and without silicate enrichment and additional enrichment with phytoplankton nutrients and high amounts of glucose (C_3 and C_{10} , and $C_3\text{Si}$ and $C_{10}\text{Si}$) (Figs. 6, 7). The main differences between C_3 and C_{10} , and $C_3\text{Si}$ and $C_{10}\text{Si}$ at the end of the study period were (1) the large biomass of bacteria $> 2 \mu\text{m}$ that was significantly higher in C_3 and C_{10} than in $C_3\text{Si}$ and $C_{10}\text{Si}$ and (2) the large diatom biomass in the Si-enriched enclosures not found in the enclosures without Si enrichment (Fig. 7). Consequently, a substantial part of the added phytoplankton nutrients were buffered in either the grazing-resistant bacteria—that is, bacterial cells $> 2 \mu\text{m}$ —or in the grazing-resistant phytoplankton cells as diatoms. In the first case, bacterial production exceeded primary production; in

the second case, primary production exceeded bacterial production (Fig. 2).

Biomass accumulations fit with the pattern in turnover time for glucose, which was significantly higher in the Si set than in the corresponding mesocosms of the no-Si set when silicate became depleted in the no-Si set (Figs. 1, 7, 8, upper panel). The trend found is consistent with the idea that bacterial consumption of glucose was inhibited because mineral nutrients, needed for bacterial growth, were channeled into grazing-resistant diatoms.

The pattern with regard to the turnover time of glucose (T_G), with rapid glucose turnover times in mesocosms C_1 and $C_1\text{Si}$ after 3 d (Fig. 8, upper panel), indicates that the system by then was able to consume the $1\times$ Redfield addition of glucose-C, and bacteria thus returned to C-limited growth in these mesocosms. The subsequent increase of T_G , indicating a slower uptake rate, in $C_1\text{Si}$ suggests that bacteria in $C_1\text{Si}$ became mineral nutrient-limited following the onset of Si addition. Following a similar interpretation, in C_3 , the rate of glucose consumption had increased sufficiently by Day 9 to consume the added glucose (Figs. 8, 9), and bacteria therefore shifted back to C-limited growth in C_3 toward the end of the experimental period. As expected in this scenario, the increase in bacterial production in C_3 stopped from Day 8 onward (Fig. 2).

In the mathematical representation analyzed by Thingstad et al. (1997), production by mineral nutrient-limited bacteria increases rapidly once the added nutrients are transferred via phytoplankton and heterotrophic nanoflagellates into microzooplankton. Within this framework of explanation, enough

of the added mineral nutrients had been transferred up the food chain to microzooplankton to deplete the added glucose around Day 3 in C₁ and around Days 8–9 in C₃, whereas the system never was able to consume all the added glucose in C₁₀. The lack of a similar increase of bacterial production in C₃Si and C₁₀Si (Fig. 2) might then be interpreted in terms of a food web in which nutrients remain sequestered in diatoms because they are not grazed by microzooplankton—a food web in which competition for mineral nutrients therefore remained severe.

Our results suggest that bacterial DOC consumption might depend not only on the degradability of DOC, but also on the structure of the microbial food web. Accumulation of DOC in the photic zone can thus be the result of a strong competition for mineral nutrients because of nutrient sequestration in grazing-resistant colony-forming algae. In the present investigation, we did not find colony-forming algae other than diatoms that competed successfully with bacteria. The characteristics of colony-forming diatoms that aid their success are cell extensions, like setae and processes that increase their effective size with regard to grazers, and vacuoles, which yield a relatively large cell surface compared to their plasma volume; a surface to plasma volume ratio which is considerably larger than that of other algae of similar size. It should also be noted that diatoms have considerably higher in situ growth rates than any other phytoplankton groups (Furnas 1990; Latasa et al. 1997). We believe our data show that because diatoms need silicate for growth, availability of silicate will not only influence competition within the phytoplankton compartment, but also competition between phytoplankton and bacterioplankton.

We found that bacteria >2 μm that form colonies 20–60 μm in diameter or that filaments up to 200 μm in length can compete successfully with algae <10 μm, but not with chain-forming diatoms. The longest diatom chains were up to 1 mm in length and consequently not available for the small neritic copepods present in the mesocosms of this investigation, whereas the colony-forming bacteria were suitable in size. Mesozooplankton feeding on bacterial aggregates has been reported by Lawrence et al. (1993). However, the lack of response in the mesozooplankton compartment (mesozooplankton biomass increased similarly in mesocosms with and without mineral nutrient enrichment, Fig. 5) could be explained by the mesozooplankton generation time that exceeded the length of the experiment. Alternatively, diatoms, which are known to have higher growth potentials than other algae (Furnas 1990), could also have higher growth potentials than colony-forming bacteria. Bacteria >2 μm with complex growth forms have considerably lower growth potentials than bacteria <2 μm and only seem to be favored when bacteria <2 μm are strongly controlled by grazers (Caron et al. 1988; Jürgens and Güde 1994; Šimek et al. 2001).

Perhaps our most significant finding was experimental confirmation of the idea that the ability of heterotrophic bacteria to consume the added source of labile DOC (glucose) can be reduced when silicate is available to diatoms. A more detailed understanding of the underlying mechanisms apparently requires a description of how mineral nutrient competition (e.g., for N, P, or Fe) and predation from different

classes of predators work in concert. Nonetheless, our results support the theoretical suggestion (Thingstad and Rassoulzadegan 1999) that major aspects of these interactions can be understood by simply adding diatoms and mesozooplankton to the idealized food webs analyzed previously (Thingstad et al. 1997, 1999a,b). Interestingly, this gives a theoretical concept where silicate and labile DOC play opposing roles by potentially restricting the flow of mineral nutrients through the “microbial” and “classical” sides, respectively, of the photic zone food web. Diatom–bacteria interactions might be more intricate and have a more important role in controlling the ocean’s C-cycle than appreciated so far.

References

- BJØRNSSEN, P. K. 1986. Automatic determination of bacterioplankton biomass by image analysis. *Appl. Environ. Microbiol.* **51**: 1199–1204.
- BLOEM, J., M. J. B. BÄR-GILISSEN, AND T. E. CAPPENBERG. 1986. Fixation, counting, and manipulation of heterotrophic nanoflagellates. *Appl. Environ. Microbiol.* **52**: 1266–1272.
- BRATBAK, G., AND T. F. THINGSTAD. 1985. Phytoplankton–bacteria interactions: An apparent paradox? Analysis of a model system with both competition and commensalism. *Mar. Ecol. Prog. Ser.* **25**: 23–30.
- CARON, D. A., J. C. GOLDMAN, AND M. R. DENNETT. 1988. Experimental demonstration of the roles of bacteria and bacterivorous protozoa in plankton nutrient cycles. *Hydrobiologia* **159**: 27–40.
- CHOI, J. W., AND D. K. STOECKER. 1989. Effects of fixation on cell volume of marine planktonic protozoa. *Appl. Environ. Microbiol.* **55**(1): 1761–1765.
- CURRIE, D. J., AND J. KALFF. 1984a. A comparison of the abilities of freshwater algae and bacteria to acquire and retain phosphorus. *Limnol. Oceanogr.* **29**: 298–310.
- , AND J. KALFF. 1984b. Can bacteria outcompete phytoplankton for phosphorus? *Microb. Ecol.* **10**: 205–216.
- , AND ———. 1984c. The relative importance of bacterioplankton and phytoplankton in phosphorus uptake in freshwater. *Limnol. Oceanogr.* **29**: 311–321.
- EGGE, J. K. 1997. Influence of silicate on particulate carbon production in phytoplankton. *Mar. Ecol. Prog. Ser.* **147**: 219–230.
- , AND D. L. AKSNES. 1992. Silicate as regulating nutrient in phytoplankton competition. *Mar. Ecol. Prog. Ser.* **83**: 281–289.
- ELSER, J. J., L. B. STABLER, AND R. P. HASSETT. 1995. Nutrient limitation of bacterial growth and rates of bacterivory in lakes and oceans: A comparative study. *Aquat. Microb. Ecol.* **9**: 105–110.
- FURNAS, M. J. 1990. In situ growth rates of marine phytoplankton: Approaches to measurement, community and species growth rate. *J. Plankton Res.* **12**: 1117–1151.
- GRASSHOFF, K., M. EHRHARDT, AND K. KREMLING [EDS.]. 1983. *Methods of seawater analysis*, 2nd ed. Verlag-Chemie.
- GUSTAFSON, D. E., JR., D. K. STOECKER, M. D. JOHNSON, W. F. VAN HEUKELEM, AND K. SNEIDER. 2000. Cryptophyte algae are robbed of their organelles by the marine ciliate *Mesodinium rubrum*. *Nature* **405**: 1049–1052.
- HARRISON, W. G., F. AZAM, E. H. RENGER, AND R. W. EPPLEY. 1977. Some experiments on phosphate assimilation by coastal marine plankton. *Mar. Biol.* **40**: 9–18.
- HAVSKUM, H., AND A. S. HANSEN. 1997. Importance of pigmented and colourless nano-sized protists as grazers on nanoplankton in a phosphate-depleted Norwegian fjord and in enclosures. *Aquat. Microb. Ecol.* **12**: 139–151.

- HILLEBRAND, H., C. D. DÜRSELEN, D. KIRSCHTEL, U. POLLINGER, AND T. ZOHARY. 1999. Biovolume calculation for pelagic and benthic microalgae. *J. Phycol.* **35**: 403–424.
- HOBBIE, J. E., AND C. C. CRAWFORD. 1969. Bacterial uptake of organic substrate: New methods of study and application to eutrophication. *Verh. Int. Ver. Limnol.* **17**: 725–730.
- JASSBY, A. D., AND T. PLATT. 1976. Mathematical formulation of the relationship between photosynthesis and light for phytoplankton. *Limnol. Oceanogr.* **21**: 540–547.
- JÜRGENS, K., AND H. GÜDE. 1994. The potential importance of grazing resistant bacteria in planktonic systems. *Mar. Ecol. Prog. Ser.* **112**: 169–188.
- LATASA, M., M. R. LANDRY, L. SCHLÜTER, AND R. R. BIDIGARE. 1997. Pigment-specific growth and grazing rates of phytoplankton in the central equatorial Pacific. *Limnol. Oceanogr.* **42**: 289–298.
- LAWRENCE, S. G., A. AHMAD, AND F. AZAM. 1993. Fate of particle-bound bacteria ingested by *Calanus pacificus*. *Mar. Ecol. Prog. Ser.* **97**: 299–307.
- MULLIN, M. M., P. R. SLOAN, AND P. W. EPPLEY. 1966. Relationship between carbon content, cell volume, and area in phytoplankton. *Limnol. Oceanogr.* **11**: 307–311.
- PENGERUD, B., E. F. SKJOLDAL, AND T. F. THINGSTAD. 1987. The reciprocal interaction between degradation of glucose and ecosystem structure. Studies in mixed chemostat cultures of marine bacteria, algae, and bacterivorous nanoflagellates. *Mar. Ecol. Prog. Ser.* **35**: 111–117.
- PORTER, K. G., AND Y. S. FEIG. 1980. The use of DAPI for identifying and counting aquatic microflora. *Limnol. Oceanogr.* **25**: 943–948.
- PUTT, M., AND D. K. STOECKER. 1989. An experimentally determined carbon: volume ratio for marine oligotrichous ciliates. *Deep-Sea Res.* **37**: 1713–1731.
- RHEE, G.-Y. 1972. Competition between an alga and an aquatic bacterium for phosphate. *Limnol. Oceanogr.* **17**: 505–514.
- RIEMANN, B., AND L. M. JENSEN. 1991. Measurements of phytoplankton primary production by means of the acidification and bubbling method. *J. Plankton Res.* **13**: 853–862.
- SANDERS, R. W., K. G. PORTER, S. J. BENNETT, AND A. E. DEBIASE. 1989. Seasonal patterns of bacterivory by flagellates, ciliates, rotifers, and cladocerans in a freshwater planktonic community. *Limnol. Oceanogr.* **34**: 673–687.
- ŠIMEK, K., AND OTHERS. 2001. Changes in bacterial community composition and dynamics and viral mortality rates associated with enhanced flagellate grazing in a mesoeutrophic reservoir. *Appl. Environ. Microbiol.* **67**: 2723–2733.
- SIMON, M., AND F. AZAM. 1989. Protein content and protein synthesis rates of planktonic marine bacteria. *Mar. Ecol. Prog. Ser.* **51**: 201–213.
- SKOOG, A., B. BIDDANDA, AND R. BRENNER. 1999. Bacterial utilization of dissolved glucose in the upper water column of the Gulf of Mexico. *Limnol. Oceanogr.* **44**: 1625–1633.
- SMITH, D. C., AND F. AZAM. 1992. A simple, economical method for measuring bacterial protein synthesis rates in seawater using ³H-leucine. *Mar. Microb. Food Webs* **6**: 107–114.
- SØNDERGAARD, M., L. M. JENSEN, AND G. ÆRTEBRJERG. 1991. Picoalgae in Danish coastal waters during summer stratification. *Mar. Ecol. Prog. Ser.* **79**: 139–149.
- STRATHMANN, R. R. 1967. Estimating the organic content of phytoplankton from cell volume or plasma volume. *Limnol. Oceanogr.* **12**: 411–418.
- SUGIMURA, Y., AND Y. SUZUKI. 1988. A high-temperature catalytic oxidation method for the determination of non-volatile dissolved organic carbon in seawater by direct injection method. *Mar. Chem.* **24**: 105–131.
- SUTTLE, C., J. FUHRMAN, AND D. CAPONE. 1990. Rapid ammonium cycling and concentration-dependent partitioning of ammonium and phosphate: Implications for carbon transfer in planktonic communities. *Limnol. Oceanogr.* **35**: 424–433.
- THINGSTAD, T. F., AND F. RASSOULZADEGAN. 1999. Conceptual models for the biogeochemical role of the photic zone microbial food web, with particular reference to the Mediterranean Sea. *Prog. Oceanogr.* **44**: 271–286.
- , E. F. SKJOLDAL, AND R. A. BOHNE. 1993. Phosphorus cycling and algal-bacterial competition in Sandsfjord, western Norway. *Mar. Ecol. Prog. Ser.* **99**: 239–259.
- , Å. HAGSTRÖM, AND F. RASSOULZADEGAN. 1997. Accumulation of degradable DOC in surface waters: Is it caused by a malfunctioning microbial loop? *Limnol. Oceanogr.* **42**: 398–404.
- , H. HAVSKUM, H. KAAS, T. G. NIELSEN, B. RIEMANN, D. LEFÈVRE, AND P. J. LE B. WILLIAMS. 1999a. Bacteria-protist interactions and organic matter degradation under P-limited conditions. Analysis of an enclosure experiment using a simple model. *Limnol. Oceanogr.* **44**: 62–79.
- , M. PÉREZ, S. PELEGRI, J. DOLAN, AND F. RASSOULZADEGAN. 1999b. Trophic control of bacterial growth in microcosms containing a natural community from northwest Mediterranean surface waters. *Aquat. Microb. Ecol.* **18**: 145–156.

Received: 22 October 2001

Accepted: 9 August 2002

Amended: 11 September 2002